Available online at www.sciencedirect.com
ScienceDirect
Journal of Magnetism and Magnetic Materials 306 (2006) 125–129
Journal of magnetism and magnetic materials
www.elsevier.com/locate/jmmm

Preparation, surface modification and microwave characterization of magnetic iron fibers

Yan Nie[a,*], Huahui He[a], Zhenshen Zhao[a], Rongzhou Gong[a], Hongbin Yu[b]

[a]*Department of Electronic Science and Technology, Huazhong University of Science and Technology, Wuhan 430074, PR China*
[b]*Department of optoelectronic Engineering, Huazhong University of Science and Technology, Wuhan 430074, PR China*

Received 17 September 2005; received in revised form 29 November 2005
Available online 23 March 2006

Abstract

In this paper, magnetic iron fibers of 3–10 μm diameter and an adjustable aspect ratio were synthesized successfully by a method involving pyrolysis of carbonyl under a magnetic field. A surface modification technology was also investigated. The electromagnetic parameters of the iron-fiber–wax composites were measured using the transmission/reflection coaxial line method in the microwave frequency range of 2–18 GHz. The results show that the prepared iron-fiber–wax composites exhibit high magnetic loss that can be further improved after phosphating. On the other hand, the complex permittivity was significantly decreased after phosphating. As a result, this kind of iron fiber may be useful for thin and lightweight radar-absorbing materials.

PACS: 42.81.Cn; 84.40.−x

Keywords: Magnetic iron fiber; Phosphating treatment; Complex permeability; Complex permittivity; Microwave

1. Introduction

The application of radar-absorbing materials can reduce the radar cross-section of the target effectively, thus contributing to the stealthy defense system [1–3]. As a result, many research groups all over the world have been studying the preparation and the electromagnetic properties of absorbers. Up to now, the most commonly used absorbers are magnetic materials (such as ferrite particles) and dielectric materials (such as carbon black particles) [4–6]. However, the expansion of applications was limited due to their thickness and weight. Recently, some research has been devoted to the study of the electromagnetic properties of nonspherical magnetic materials [1,7–10]. Some kinds of metal fibers have been produced by bundle drawing, shatter machining, and melt extracting [11–15]. All these works show that they exhibit higher permeability and hence better absorption in the radar band. But all these methods are not suitable for producing fibers with a diameter down to several micrometers, which can be detrimental to the further increase in the permeability according to the analysis in Ref. [9]. In this paper, a novel technology based on pyrolysis of carbonyl and the application of a magnetic field has been put forward to produce magnetic iron fibers. The magnetic iron fibers with diameter of 3–10 μm and an adjustable aspect ratio were prepared. Such a method proved to have the ability of large amount production. Furthermore, a surface modification technology was also adopted to improve the electromagnetic property and had been proved to be effective.

2. Experiments

2.1. Preparation technique

The assembled laboratory preparation set-up is shown in Fig. 1.

Liquid $Fe(CO)_5$ is used as the source of the iron element. First, it is heated to 140 °C by an oil-bath and, hence is converted into $Fe(CO)_5$ vapor. Then, the produced vapor is

*Corresponding author. Tel.: +86 27 87542494x808; fax: +86 27 87547337.
E-mail address: nieyanko@yahoo.com.cn (Y. Nie).

0304-8853/$ - see front matter © 2006 Elsevier B.V. All rights reserved.
doi:10.1016/j.jmmm.2006.02.233

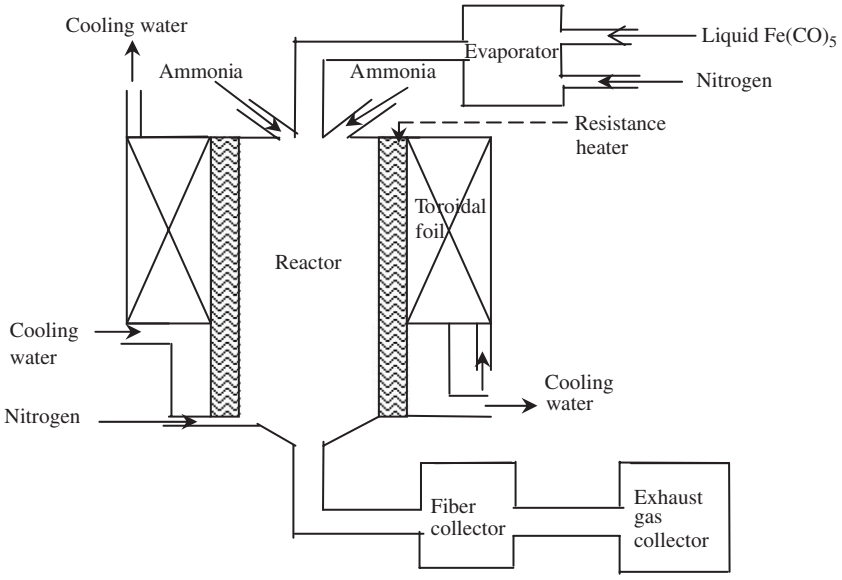

Fig. 1. The schematic diagram of iron fiber preparation set-up.

Table 1
Process parameters

Parameter	Value
$Fe(CO)_5$ vapor flow	500 ml/h
Nitrogen flow	150 ml/h
Ammonia flow	150 ml/h
Magnetic field	11000 A/m
Actor temperature	350 °C

introduced into the reactor from the top using nitrogen as the carrier gas. Meanwhile, ammonia is also added into the reactor simultaneously through two different inlets lying in the top part, diluting the vapor and controlling the composition of the prepared fibers. The chamber temperature is raised to 350 °C by using the resistance heater arranged around the side wall. In this hot environment, the vapor decomposition takes place as shown in Eq. (1). After the agglomeration and nucleation stages, the formed iron elements adhere to one another under a constant magnetic field along the vertical axis of the reactor, which is provided by the toroidal coil. Finally, the chain-shaped magnetic iron fibers are produced. Some specific parameters used in the process are described in Table 1.

$$Fe(CO)_5(g) \xrightarrow{350\,^{\circ}C} Fe(s) + 5CO(g). \quad (1)$$

2.2. Surface modification technique

The complex permittivity of the fiber–wax composite sample presents a high value (both the values of ε' and ε'' higher than 100 at 2 GHz as discussed below), compared with those of other magnetic inclusions (ferrite, iron, cobalt, permalloy, iron-coated multiwall carbon nanotubes, etc.), which are lower than 100 over the whole investigation band [16–18]. Too high values of ε' and ε'' may bring about the mismatch of normalized input impedance and reduce the absorption property in radar band [19]. Thus, a phosphating process technique is put forward to solve this problem. The treatment flow is shown schematically in Fig. 2. The solution used is mainly made up of sodium dihydrogen phosphate (NaH_2PO_4) and phosphorous acid (H_3PO_4) with concentrations 49.5 g/l and 2 ml/l, respectively, and the pH value of the solution controlled between 4 and 5. At the beginning of the process, the solution is heated to 28 °C, and then the fibers are added accompanied by solution agitation. After 1 min treatment, the fibers are extracted out of the solution by using magnetic separating technology and then dried in a vacuum.

2.3. Characterization techniques

The morphology of magnetic iron fibers was observed by Philips XL-30TMP scanning electron microscope (SEM). The transmission/reflection method was adopted to determine the relative complex permeability μ and permittivity ε of the magnetic material–wax composites using an HP8722ES vector network analyzer system [20]. The magnetic fillers were randomly dispersed in the wax with a different volume fraction. The cylindrical toroidal samples were fabricated. The samples were 3 mm in inner diameter, 7 mm in outer diameter, and 3–3.5 mm in thickness.

3. Results and discussion

Fig. 3 shows the SEM of the typical fibers prepared by the proposed technique. It can be seen from graphs (a) and

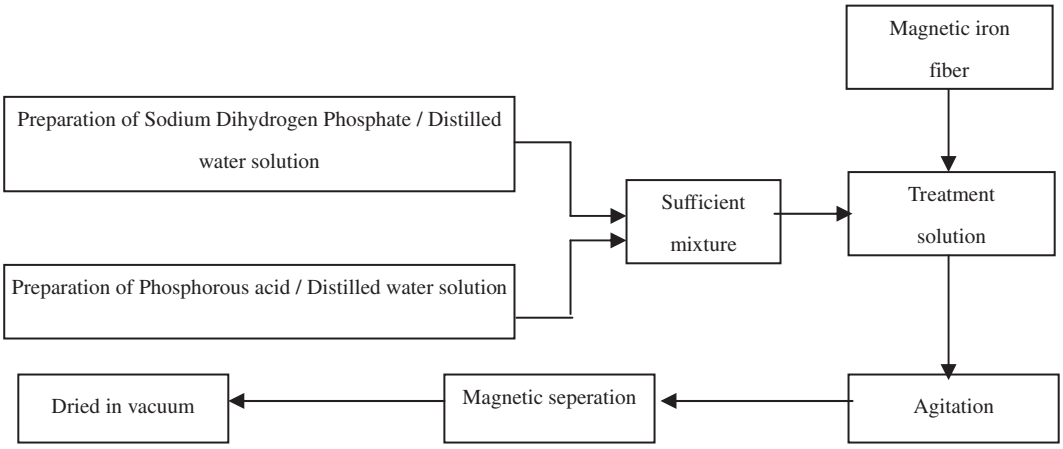

Fig. 2. The phosphating process flow.

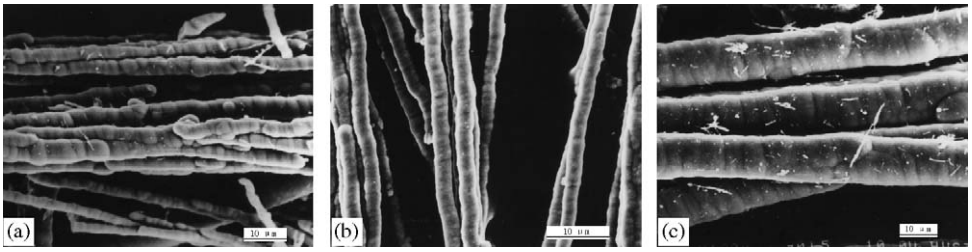

Fig. 3. Scanning electron micrographs of the prepared fibers.

(b) that the fibers appear to be chain-shaped with about 3 μm diameter, a narrow dimension distribution, and good dispersion. The diameter and the aspect ratio can be adjusted by changing the process parameters. Fig. 3(c) shows the prepared iron fiber with a diameter of about 10 μm. Furthermore, the length of the fibers can be controlled from micrometers to millimeters by changing the actor temperature and the velocity of the vapor and gas flow.

The coaxial sample A1 was prepared by mixing the iron fibers with wax at a volume content of 50%. The diameters of the fibers used here are about 3 μm.

Fig. 4 indicates that the value of μ'' is as high as 3.5 at 2 GHz indicating higher magnetic loss, while the real part of the permeability (μ′) of composite A1 also reaches 3.6 at 2 GHz over the whole investigated band and it can be inferred that they present larger values in the lower frequency range. Meanwhile, the complex permittivity (ε′,ε″) is very high in the frequency range. It is also shown in Fig. 4 that both the complex permeability and permittivity of composite A1 decrease with the increasing frequency, and the magnitude of change in lower frequency range are larger than that in the higher frequency range. The theoretical analysis of the complex permeability and permittivity was carried out in Ref. [21] and similar phenomena were reported in Ref. [22], where they were considered to be due to eddy current loss and ferromagnetic resonance.

Although possessing the better magnetic property with large filling fraction, the complex permittivity of composite A1 is too high for radar absorption applications. Ref. [19] states that too high values of ε′ and ε″, compared to the values of μ′ and μ″, can reduce the absorption property in radar band. This disadvantage can be overcome by decreasing the filling fraction. But it always works at the cost of decreasing the magnetic loss. This paper presents the phosphating process technique to overcome this disadvantage. The results for iron-fiber–wax composite A2 and phosphated iron-fiber–wax composite A3 are illustrated in Fig. 5. Both composites have the same volume fraction of 30%.

Both the complex permittivity and permeability of composite A2 are reduced, compared to those of composite A1, as shown in Fig. 4, in the whole test frequency range after reducing the filling fraction. Especially, the complex permittivity has been reduced significantly. The decrement of permittivity with cutting down the filling fraction is due to the decreasing conductivity. Compared to reducing the filling fraction, it can be seen from Fig. 5 that ε′ and ε″ can be decreased further after phosphating. Furthermore, it is very interesting that the enhancement of the value of μ″ is evident, and its value reaches 5.2 at 2 GHz and remains above 1.0 over the 2–10 GHz frequency range, which indicates higher magnetic loss after phosphating. The value of μ′ decreases slightly in the frequency range 2–7 GHz, but exhibits a tendency to increase in the higher frequency

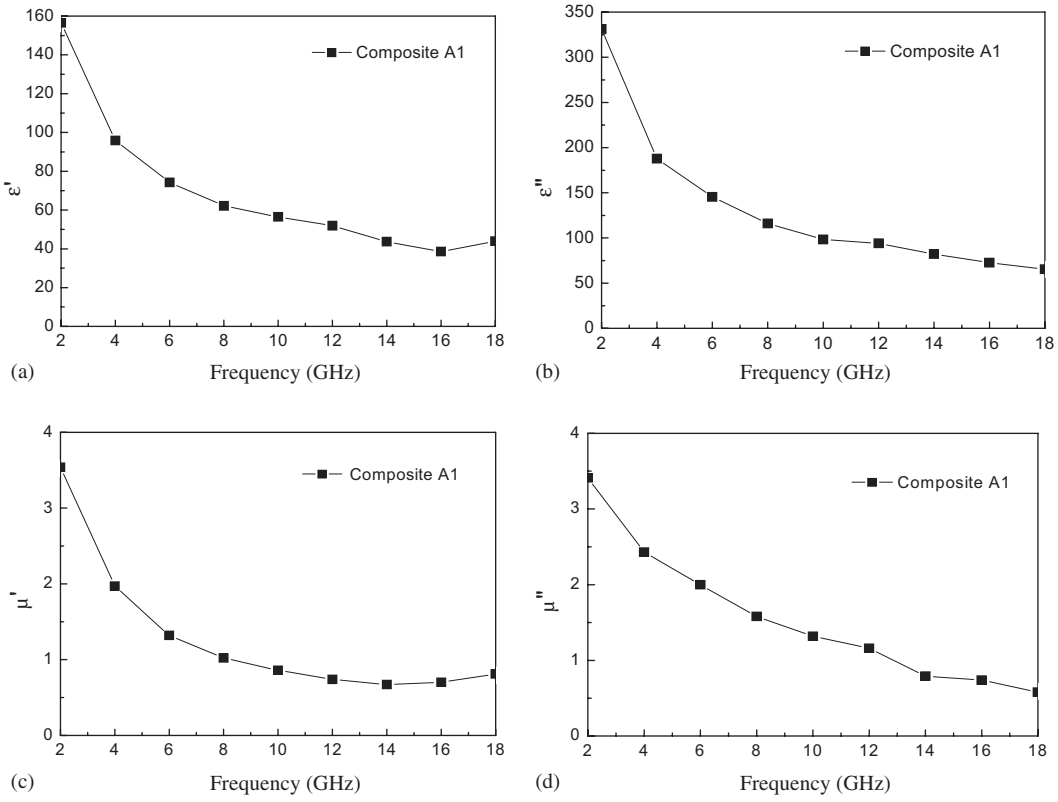

Fig. 4. Complex permittivity and permeability of composites A1 versus frequency: (a) the real part of the permittivity, (b) the imaginary part of the permittivity, (c) the real part of the permeability, and (d) the imaginary part of the permeability.

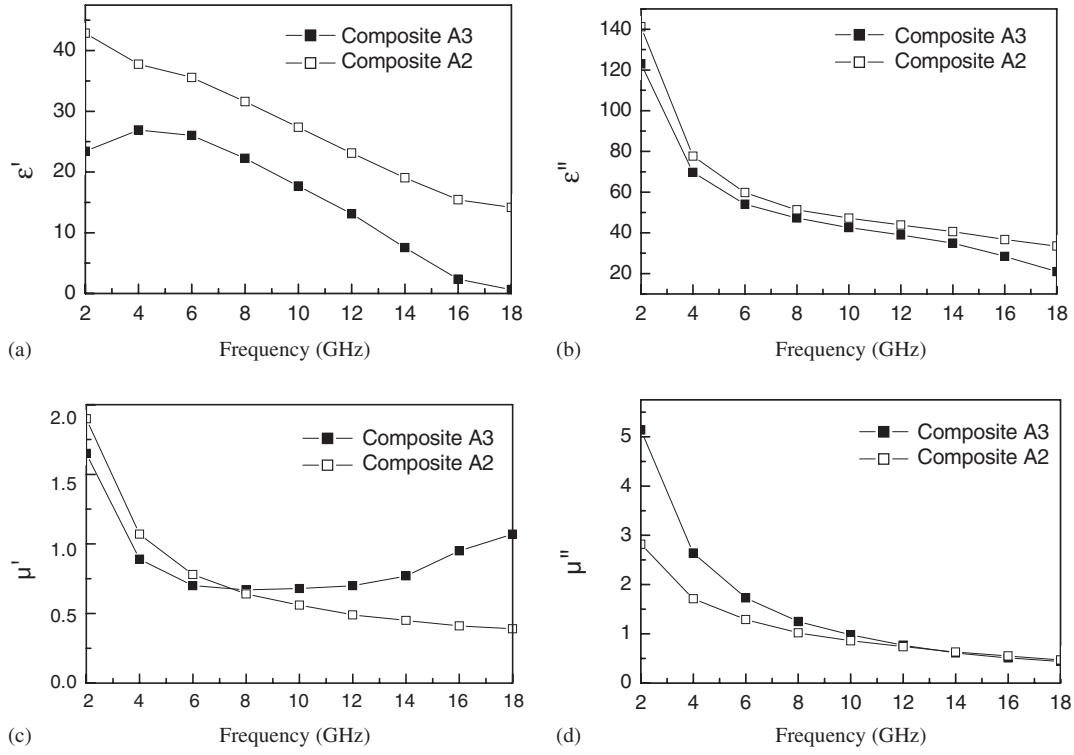

Fig. 5. Complex permittivities and permeabilities of composites A2 and A3 versus frequency: (a) the real part of the permittivity, (b) the imaginary part of the permittivity, (c) the real part of the permeability, and (d) the imaginary part of the permeability.

range, which is beneficial to the improvement of the absorbing performance in this frequency range.

According to the theory about phosphating, the reaction, as expressed in Eq. (2), takes place in the solution during the treatment [23].

$$4Fe + 4NaH_2PO_4 + 3O_2 \rightarrow 2FePO_4 \downarrow + Fe_2O_3 \downarrow + 2Na_2HPO_4 + 3H_2O. \quad (2)$$

The iron element on the fiber surface is partly converted into iron phosphate and ferric oxide through the phosphating treatment, which contribute to the reduction of the permittivity. The reduction of the conductivity also results in the increase of permeability [21].

4. Conclusions

Magnetic iron fibers with diameters down to 3 μm have been successfully prepared by using the method involving pyrolysis of carbonyl under a magnetic field. They possess a narrow diameter distribution and a low degree of agglomeration. This method has the ability of large amount production. The diameter and aspect ratio of the fibers can be controlled by changing the process parameters. In addition, this method can also be extended to prepare Ni fibers or NiFe alloy fibers. The results measured at microwave frequencies show that the values of μ' and μ'' for the iron-fiber–wax composite reach 3.6 and 3.5 at 2 GHz, respectively. A surface modification based on the phosphating process has also been discussed for fibers to improve the material property. The measurements indicate that the complex permittivity could be effectively reduced after cutting down the volume fraction of the fiber in the composite and could be further reduced after the phosphating process. Also, the magnetic loss is improved evidently due to the part conversion of the iron element into iron phosphate and ferric oxide. The resulting low permittivity and high magnetic loss can be used to achieve high absorption.

References

[1] M.Z. Wu, H.H. He, Z.S. Zhao, X. Yao, J. Phys. D 33 (2000) 2398.
[2] K.J. Vinoy, R.M. Jha, Radar Absorbing Materials From Theory to Design and Characterization, Kluwer, Norwell, 1996, pp. 13–15.
[3] H.M. Musal Jr., H.T. Hahn, IEEE Trans. Magn. 25 (1989) 3851.
[4] K. Lim, M. Kim, K. Lee, C. Park, IEEE Trans. Magn. 39 (2003) 1836.
[5] K. Ishino, Y. Narumity, Am. Ceram. Soc. Bull. 66 (1987) 1469.
[6] J. Shin, J. Oh, IEEE Trans. Magn. 29 (1993) 3437.
[7] M. Matsumoto, Y. Miyata, IEEE Trans. Magn. 33 (1997) 4459.
[8] C.E. Boyer, E.J. Borchers, R.J. Kuo, C.D. Hoyle, US Patent Specification 5085931, 1992, pp 1–10.
[9] M.Z. Wu, H.H. He, Z.S. Zhao, X. Yao, J. Magn. Magn. Mater. 217 (2000) 89.
[10] R.C. Pullar, S.G. Appleton, A.K. Bhattachacharya, J. Mater. Sci. Lett. 17 (1998) 973.
[11] R.D. Bruyne, Adv. Mater. Proc. 147 (1995) 33.
[12] G.T. Liu, Rare Met. Mater. Eng. 23 (1994) 7.
[13] J.O. Strom-Olsen, Mater. Sci. Eng. A 178 (1994) 239.
[14] P. Rudkowski, G. Rudkowska, A. Zaluska, J.O. Strom-Olsen, IEEE Trans. Magn. 28 (1992) 1899.
[15] P. Rudkowski, G. Rudkowska, J.O. Strom-Olsen, J. Appl. Phys. 69 (1991) 5017.
[16] L. Olmedo, G. Chateau, C. Deleuze, J.L. Forveille, J. Appl. Phys. 73 (1993) 6992.
[17] M.Z. Wu, H.J. Zhang, X. Yao, L. Zhang, J. Phys. D 34 (2001) 889.
[18] X. Shen, R.Z. Gong, Y. Nie, J.H. Nie, J. Magn. Magn. Mater. 288 (2005) 397.
[19] E. Michielssen, J. Sajer, S. Ranjithan, R. Mittra, IEEE Trans. Microwave Theory Tech. 41 (1993) 1024.
[20] IEEE Standards 1128-1998 IEEE recommended practice for radio-frequency (RF) absorber evaluation in the range of 30 MHz to 5 GHz, The Institute of Electrical and Electronics Engineers, Inc., New York, 1998, pp. 28–32.
[21] M.Z. Wu, Z.S. Zhao, H.H. He, J. Funct. Mater. 30 (1999) 91.
[22] M.Z. Wu, H.H. He, Z.S. Zhao, X. Yao, J. Phys. D 33 (2000) 2927.
[23] H.B. Yu, Z.S. Zhao, Y. Nie, L.W. Deng, Surf. Tech. 31 (2002) 45.